1-2010

Medial septal beta-amyloid 1-40 injections alter septo-hippocampal anatomy and function

Luis V. Colom
The University of Texas Rio Grande Valley

María Teresa Castañeda Licón
The University of Texas Rio Grande Valley

C. Banuelos

Gustavo Puras

Antonio García-Hernández

See next page for additional authors

Recommended Citation

Colom, L. V., Castañeda, M. T., Bañuelos, C., Puras, G., García-Hernández, A., Hernandez, S., Mounsey, S., Benavidez, J., & Lehker, C. (2010). Medial septal beta-amyloid 1-40 injections alter septo-hippocampal anatomy and function. Neurobiology of aging, 31(1), 46–57. https://doi.org/10.1016/j.neurobiolaging.2008.05.006

Published in final edited form as:
Neurobiol Aging. 2010 January ; 31(1): 46–57. doi:10.1016/j.neurobiolaging.2008.05.006.

Medial septal β-amyloid 1–40 injections alter septo-hippocampal anatomy and function

Luis V. Colom[1,2,*], **Maria T. Castañeda**[1], **Cristina Bañuelos**[1], **Gustavo Puras**[1], **Antonio García-Hernández**[1], **Sofia Hernandez**[1], **Suzanne Mounsey**[1], **Joy Benavidez**[1], and **Claudia Lehker**

[1] Department of Biological Sciences at the University of Texas at Brownsville/Texas Southmost College, 80 Fort Brown, Brownsville, Texas 78520 USA

[2] Center for Biomedical Studies

Abstract

Degeneration of septal neurons in Alzheimer's disease (AD) results in abnormal information processing at cortical circuits and consequent brain dysfunction. The septum modulates the activity of hippocampal and cortical circuits and is crucial to the initiation and occurrence of oscillatory activities such as the hippocampal theta rhythm. Previous studies suggest that amyloid β peptide (Aβ) accumulation may trigger degeneration in AD. This study evaluates the effects of single injections of Aβ 1–40 into the medial septum. Immunohistochemistry revealed a decrease in septal cholinergic (57%) and glutamatergic (53%) neurons in Aβ 1–40 treated tissue. Additionally, glutamatergic terminals were significantly less in Aβ treated tissue. In contrast, septal GABAergic neurons were spared. Unitary recordings from septal neurons and hippocampal field potentials revealed an approximately 50% increase in firing rates of slow firing septal neurons during theta rhythm and large irregular amplitude (LIA) hippocampal activities and a significantly reduced hippocampal theta rhythm power (49%) in Aβ 1–40 treated tissue. Aβ also markedly reduced the proportion of slow firing septal neurons correlated to the hippocampal theta rhythm by 96%. These results confirm that Aβ alters the anatomy and physiology of the medial septum contributing to septo-hippocampal dysfunction. The Aβ induced injury of septal cholinergic and glutamatergic networks may contribute to an altered hippocampal theta rhythm which may underlie the memory loss typically observed in AD patients.

Keywords

Septo-hippocampal; amyloid; glutamatergic; cholinergic; GABAergic; septum

1. Introduction

Alzheimer's disease (AD) is an age-related progressive disorder of the brain that leads to memory loss, dementia and, ultimately death. Although AD was described a century ago, the

*Corresponding Author: Luis V. Colom, M.D., Ph.D. Department of Biological Sciences, 80 Fort Brown, Brownsville Texas 78520, Phone: (956) 882-5048, Fax: (956) 882-5043 Fax. luis.colom@utb.edu.

5.1 Disclosures Statement

There are no actual or potential conflicts of interest for any of the authors.

molecular mechanisms underlying neuronal dysfunction and degeneration are still unclear. The brain of an individual with AD exhibits extracellular senile plaques of aggregated amyloid-β-peptide (Aβ) and a profound loss of basal forebrain cholinergic neurons that innervate the hippocampus and the neocortex (Whitehouse et al, 1982; Selkoe 2000;Hardy and Selkoe, 2002). This loss of basal forebrain cholinergic neurons led to the cholinergic hypothesis of AD which states that basal forebrain cholinergic neurons are severely affected in the course of the disease and that the resulting cerebral cholinergic deficit leads to memory loss and other cognitive symptoms, which are characteristic of AD (Davies and Maloney, 1976; Pearson et al, 1983; Schliebs, 2005). Recent studies have shown an association between a decline in learning and memory and a deficit in excitatory amino acid neurotransmission. This deficit accompanies the impairment of the cholinergic system which modulates glutamatergic neurotransmission by targeting the neocortical and hippocampal glutamatergic pyramidal neurons (Francis *et al*., 1999). Thus, AD neurological decline may be attributed to cholinergic hypofunction, as described in the cholinergic hypothesis, in combination with the loss of excitatory glutamatergic function (Francis *et al.*, 1999).

The septum and the hippocampus are heavily interconnected through the fimbria-fornix and are functionally coupled (Bland and Colom, 1993), often referred to collectively as the septo-hippocampal system (Colom, 2006). The septo-hippocampal projection includes well-known cholinergic and GABAergic components (Lynch *et al.*, 1977; Kohler *et al.*, 1984; Bland and Colom, 1993). Recent electrophysiological and anatomical studies have shown that a subpopulation of septal glutamatergic neurons projects to the hippocampus (Sotty *et al.*, 2003; Hajszan *et al*., 2004; Manseau *et al*., 2005), constituting 23% of the septo-hippocampal projection (Colom *et al.*, 2005). Hence, the septo-hippocampal projection is a three neurotransmitter pathway.

The synchronized depolarization of hippocampal neurons produces field potentials in a frequency range of 3–12 Hz typically referred to as theta rhythm (Bland and Colom, 1993). Several lines of evidence indicate that the septum plays a critical role in hippocampal theta rhythm generation (Morales *et al.* 1971; Colom and Bland 1991; Bland and Colom, 1993; Lee *et al.*, 1994; Vinogradova, 1995; Bland *et al.*, 1999). Furthermore, the occurrence of hippocampal theta rhythm depends on the proportion of septal neurons involved in the rhythmic process while the frequency of the theta field activity is determined by the frequency of the rhythmical "theta" bursts in septal neurons (Bland and Colom, 1993; Vinogradova, 1995; Bland *et al.*, 1999). Septal lesions, in addition to blocking theta, produce severe impairments in memory processes (Winson, 1978; Vinogradova, 1995). The hippocampal theta rhythm appears to act as a windowing mechanism for synaptic plasticity (Huerta and Lisman, 1993). Theta also plays a role in the neural coding of place (Winson, 1978; O'Keefe, 1993). Theta also seems to play a role in sensory-motor integration (Bland and Oddie, 2001).

Human theta oscillations occur during exploratory search and goal-seeking behaviors as well as during virtual movement when sensory information and motor planning are both in flux but not during periods of self-initiated stillness (Caplan et al. 2003). Movement-related theta oscillations are observed in human hippocampus and cortex, suggesting that both structures play a role in sensorimotor integration (Ekstrom et al., 2005). This suggests that experimental data regarding Aβ-induced hippocampal theta rhythm alterations in rats is important in understanding sensorimotor processing in human patients suffering from AD.

In vitro, medial septal neurons have been classified according to their firing patterns and membrane properties as slow-firing, fast-firing, regular-firing or burst-firing (Jones *et al.*, 1999; Henderson *et al.*, 2001; Garrido *et al.*, in press). These electrophysiologically characterized septal neurons have been identified *in vitro* using single cell reverse transcriptase polymerase chain reaction (RT-PCR). While cholinergic neurons typically display slow-firing

phenotypes, most GABAergic neurons display fast- and burst-firing phenotypes. In contrast, glutamatergic neurons display heterogeneous firing properties, including slow-firing phenotypes (Sotty *et al.*, 2003; Manseau *et al.*, 2005).

In animal models of AD, Aβ peptide 1–42 injections into the medial septum injured neurons. Most neurons damaged by Aβ were choline acetyltransferase (ChAT) positive, while only minor effects of Aβ were observed on parvalbumin (PV) positive neurons (putative GABAergic) (Harkany *et al.*, 1995). The effect of Aβ on glutamatergic septal neurons is not known due largely to the fact that a significant septal glutamatergic neuronal population was only recently described.

Glutamatergic actions in other regions of the brain show that glutamate mediates most excitatory synaptic transmission in the brain. In addition, synaptic strength at glutamatergic synapses shows a remarkable degree of use-dependent plasticity which may represent a physiological correlate to learning and memory (McGee and Bredt, 2003). Septal glutamatergic neurons are well posed to control hippocampal excitability and rhythmical activities (e.g., theta rhythm) that promote synaptic plasticity. Cholinergic mechanisms modulate glutamatergic synapses and, through this action, learning and memory formation (Jerusalinsky *et al.*, 1997). Glutamatergic neurons, together with basal forebrain cholinergic neurons, constitute the two neuronal systems highly vulnerable to AD (Francis *et al.*, 1999; Bell and Cuello, 2006). Aβ-induced damage of septal glutamatergic neurons may play a central role in AD. While glutamate actions in various areas of the brain are well characterized, little is known about septal glutamatergic neurons and their alterations induced by age-related pathologies such as AD. Therefore, to investigate the effects of amyloid, an indicator of AD, on all three septal neuronal populations, septal networks and septohippocampal function, we administered single injections of Aβ 1–40 into the medial septum. Subsequently, electrophysiological recordings of hipopocampal theta rhythm and immunohistochemistry were used to assess anatomical and electrophysiological alterations.

2. Materials and Methods

2.1 Animals

Adult male Sprague Dawley rats (n= 50; 250–350 g; Harlan) were housed and maintained on a 12/12-h light/dark cycle and provided food and water ad libitum. All animal protocols used in this study were in compliance with the National Institutes of Health Guide for the Care and Use of Laboratory Animals and approved by the Institutional Animal Care and Use Committee of UTB/TSC. All surgical procedures and perfusions were performed with a ketamine-based anesthetic (ketamine: 42.8mg/ml, xylazine: 8.6 mg/ml and acepromazine: 1.4 mg/ml in saline; 1 ml/kg).

2.2 Aβ Septal Injections

Synthetic Aβ peptide 1–40 (Bachem Torrance, California) and Aβ peptide 40-1(Bachem Torrance, California), a reverse peptide used as a control, were separately dissolved in 0.01 M phosphate-buffered saline (PBS) at a concentration of 2 μg/μl and incubated at 37 °C for one week before use as described by Gonzalo-Ruiz and Sanz (2002) to allow aggregation of fibrils. Atomic force microscopy was used to verify that incubated Aβ 1–40 contained soluble oligomers before injections (Figure 1A, B).

Anesthetized animals received a single injection into the medial septum by means of a stereotaxic apparatus (coordinates: AP=0.5, L=.2, V=−6.5 from the dura) (Figure 1C). Four microliters of Aβ 1–40, Aβ 40-1, or PBS were injected with a 10-μL Hamilton syringe and the needle kept in place for fifteen minutes before withdrawing. Ten to 15 animals were prepared

for each experimental group (Aβ 1–40, Aβ 40-1 and PBS). Animals were allowed a one week recovery period in their original housing environment prior to acute electrophysiological procedures.

2.3 Electrophysiology

Animals were initially anesthetized with Isoflurane (The Butler Company, Dublin, OH) while a jugular cannula was inserted. Isoflurane was then discontinued and Urethane (Sigma-Aldrich, St. Louis, MO), 0.8 g/ml was administered via the jugular cannula to maintain an appropriate level of anesthesia during the remaining surgical and experimental procedures. The rats were placed in a stereotaxic instrument (David Kopf Instruments, Tujunga, CA) with the plane between bregma and lambda horizontally leveled. Body temperature was maintained at 37°C with a self regulating heating pad (Fine Science Tools Inc., Foster City, CA). An uninsulated silver wire (Sigma-Aldrich, St. Louis, MO) placed in the cortex, anterior to bregma served as an indifferent electrode. Another insulated stainless steel wire for recording hippocampal field activity was placed in the right dorsal hippocampal formation in the dentate molecular layer (3.8 mm posterior to bregma, 2mm lateral to the midline and 2.5 mm ventral to the dural surface). To show that theta amplitude was not due to the electrode position, the point of maximum theta amplitude was found in each experiment as described in previous work (Bland and Colom 1993; Bland et al. 1999). Medial septum diagonal band of Broca (MS-DBB) recordings were made 0.5mm anterior to bregma, 0.0–0.5 mm lateral to the midline, and ventral 5.2–7.2 mm from the dural surface. Cells were recorded with glass microelectrodes (15–30 MΩ) filled with 0.5 M sodium acetate. Hippocampal and septal microelectrodes were carried in independent microdrives, Electrode Manipulator Model 960 (David Kopf Instruments, Tujunga, CA) and a CMA-12CC actuator (Newport Corporation, Irvine, CA), respectively.

2.4 Histology

Animals (n=35) were deeply anesthetized and perfused intracardially with 0.1 M phosphate-based buffer saline (PBS) (pH 7.4) followed by a fixative solution containing 4% paraformaldehyde and 0.1% glutaraldehyde in 0.1 M PBS. Brains were removed, post-fixed in the same fixative solution overnight and then cryoprotected in 30% sucrose. Thirty μm slices were cut using a cryostat. Only brains with confirmed medial septal injection sites were used in this study. Free floating sections were stored at 4°C in well plates containing PBS until processed for immunohistochemistry. Sections surrounding the injection site were mounted and processed for Thioflavine S to confirm the presence of Aβ deposits (Figure 1D). Trajectories of electrodes used in electrophysiological recordings of theta rhythm in the hippocampus were confirmed with Cresyl violet staining. Only recordings from animals with confirmed hippocampal electrode trajectories were included in this study (n=183).

2.5 Immunohistochemistry

Free floating immunohistochemistry was performed on Aβ 1–40 treated and control tissue (Aβ 40-1 and PBS) in order to visualize neuronal populations in the medial septum. Briefly, medial septal sections were incubated for 10 min in 0.3% H_2O_2 to inhibit endogenous peroxidase activity. Non-specific staining was blocked by incubating tissue in 10% bovine serum albumin (BSA) for 1 hour at room temperature. Sections were incubated overnight in primary antibodies at room temperature. A mouse anti-NeuN antibody (1:1000, Chemicon) which stains neuronal nuclei was used to reveal the overall number of neurons. GABAergic and cholinergic neurons were visualized using a mouse anti-GAD67 antibody (1:1000, Chemicon) and a goat anti-ChAT antibody (1:200, Chemicon), respectively. Glutamatergic populations were revealed using a mouse anti-glutamate antibody (1:3000, Immunostar). Glutamatergic terminals were visualized using guinea pig anti-VGLUT1 (1:2000) and anti-VGLUT2 (1:4000) antibodies (Chemicon). Following primary antibody incubation, sections

were incubated at room temperature for 2 hours in their respective biotinylated secondary antibodies (1:200), NeuN labeling: goat anti-mouse (Vector), GABAergic labeling: goat anti-mouse (Vector), cholinergic labeling: donkey anti-goat (Vector), glutamatergic labeling: goat anti-mouse (Vector). Finally, sections were incubated in avidin-biotin complex (ABC, Vector) for 1 hour. Neuronal populations were revealed using the chromogen 3-3′diaminobenzidine (DAB, Vector). In each experiment some sections were incubated without the primary antibody to determine staining specificity. Sections were mounted onto gelatin-coated slides, dehydrated in graded ethanol, cleared in xylene and coverslipped for further analysis.

2.6 Digital Imaging and Quantification

Bright field images were captured using an Axiovert 200 microscope (Zeiss) equipped with an Optronics CCD camera coupled to StereoInvestigator software (MBF BioScience). Contours of the medial septal region were determined using the corresponding sections of the stereotaxic atlas of the rat brain (Paxinos and Watson, 1998). The area of the contour and the number of cells within each contour was determined using the meander scan function in StereoInvestigator. Cell density was calculated by dividing the number of cells by the area of the contour in which the cells were located. Glutamatergic terminals (VGLUT1 and VGLUT2) were estimated using the optical fractionator probe in StereoInvestigator.

2.7 Data acquisition, analysis and firing pattern classification

Brain signals were displayed, digitized, and sampled at a frequency of 10 KHz with a 12-bit DT-2839 A/D board and SciWorks 3.0 SP1 (DataWave Technologies, Longmont, CO), and recorded for off-line analysis. Electroencephalographic (EEG) signals were amplified and filtered on-line (low-pass at 100 Hz) using an AC/DC amplifier (3000 model, A-M Systems, Inc., Carlsborg, WA). Cell recordings were amplified and filtered on-line (low-pass at 2000 Hz, high-pass at 500 Hz) using a NEURODATA IR-183A recording amplifier and a FLA-01 filter/amplifier (Cygnus Technology, Inc. Delaware Water Gap, PA). Hippocampal field potentials and septal cell discharges were simultaneously recorded during four hippocampal field conditions: (1) LIA only, (2) transition from LIA to theta, (3) theta only, and (4) transition from theta to LIA. Stable cell recordings were made for an average of 30 min to insure that a minimum of 5–10 30-second transitions were acquired for analysis. Each EEG was subjected to a fast Fourier analysis, Clampfit 9.2 (Molecular Devices, CA), and classified as either theta or LIA by the following criteria: (1) the theta rhythm functional state was defined as a sinusoidal-like waveform with a peak frequency of 3–8 Hz and a small bandwidth, and (2) the “LIA” functional state was defined as a large amplitude irregular activity with a broad frequency band (0.5–25.0 Hz) (Leung et al. 1982). Analysis of cell recordings (30 sec) using Clampfit 9.2 software (Molecular Devices) provided the mean, firing frequency (Hz), action potential duration (ms), and amplitude (mV). Septal neurons were classified as either slow-firing or fast-firing as described by previous studies (Brazhnik and Fox 1997, 1999; Sotty et al. 2003, Colom et al. 2006). Septal units having a mean firing frequency < 12 Hz were considered slow firing neurons and units having a mean firing frequency ≥ 12 Hz were considered fast-firing neurons. Firing periodicity (rhythmicity) was examined using autocorrelation analysis. Rhythmical units showed periodicity in their autocorrelations (Bland and Colom 1993). Cross-correlograms were used to determine whether septal units and hippocampal θ rhythm recordings were related (SciWorks 3.0 SP1 software).

2.8 Statistical analysis

Mean cell densities of each neuronal population were compared amongst Aβ1–40, Aβ 40-1 and PBS treated rats using a one-way analysis of variance (ANOVA). ANOVA analysis was followed by Tukey’s post hoc analysis. Significant differences for all statistical testing were defined by a *p* value of less than 0.05. Numerical data is represented as means and standard

errors (S.E.M.). All statistical tests were performed using statistical analysis software (SPSS 14.0, SPSS, Inc., Chicago, Illinois).

Mean cell firing frequencies and hippocampal theta rhythm power spectrum values were compared amongst the three groups (Aβ1–40, Aβ 40-1, and PBS) using the Kruskal-Wallis test. To find if there was a statistically significant reduction in the numbers of recorded neurons in the three groups, the Difference in Proportions Test for Two Independent Proportions was used. Significant differences for all statistical testing were defined by a *p* value of less than 0.05. All statistical tests were performed using StatsDirect 2.6.6 statistical software.

3. Results

3.1 Histology

Aβ deposits were detectable at the injection site of Aβ 1–40 treated tissue as verified by Thioflavine S staining (Figure 1) and Congo Red (not shown) while no amyloid deposits were detectable in Aβ 40-1 and PBS treated tissue (not shown). Cells with glial morphology were visible near the injection site in stained tissue of all experimental groups (Aβ 1–40, Aβ 40-1, PBS). However, glia was visibly more extensive in Aβ 1–40 treated tissue (not shown). This glial reaction is consistent with previous studies (Giovannelli, et al. 1995,Scali., et al. 1999).

3.2 Aβ 1–40 produces an overall reduction in septal neurons

Analysis of NeuN-positive neuronal cell density in all groups revealed a significant decrease in NeuN positive neurons in Aβ 1–40 treated tissue (28%, p= 0.021) compared to control groups (PBS treated tissue), indicating an overall reduction of septal neurons (Figures 2, 3A–C). There was no significant difference between the cell densities of PBS treated tissue and tissue treated with Aβ 40-1 (Table 1).

3.3 Aβ 1–40 selectively injures cholinergic and glutamatergic septal neurons

Cholinergic neuronal density assessed by ChAT staining of somas was significantly reduced by 57% compared to PBS controls (p=.001) (Table 1, Figures 2, 3D–F). Additionally, glutamatergic neuronal density assessed by glutamate staining was significantly decreased by 53% compared to controls (p=.001) (Table 1, Figures 2, 3G–L). In contrast, populations of GABAergic neurons assessed by GAD67 immunoreactivity were not significantly reduced (Table 1). Thus, Aβ 1–40 selectively injures cholinergic and glutamatergic medial septal neurons while sparing medial septum GABAergic neurons. No significant differences were found between PBS and Aβ 40-1in these neuronal populations (Table 1).

3.4 Aβ 1–40 significantly reduces glutamatergic terminals in the medial septum

Glutamatergic terminals assessed by VGLUT1 and VGLUT2 punctate immunoreactivity were significantly reduced following Aβ 1–40 injections into the medial septal region (Figures 4–5). VGLUT1 terminals were reduced by 21% compared to PBS controls (p=.001) (Figures 4, 5A–C). VGLUT 2 terminals were reduced by 40% compared to PBS controls (p=.001) (Figures 4, 5D–F). In control tissue, the density of VGLUT 2 immunoreactive punctate was significantly more abundant than VGLUT1 punctate which is in agreement with previous studies (Hajszan et al, 2004). While both VGLUT1 and VGLUT2 puncta were reduced in Aβ 1–40 tissue, VGLUT2 terminals in the medial septum were more affected than VGLUT1 terminals.

3.5 Aβ 1–40 altered the firing pattern of slow firing neurons

The mean firing rate of slow firing septal neurons was significantly higher in Aβ 1–40 treated animals when compared to PBS and Aβ 40-1 control animals (Fig. 6A). In Aβ 1–40 treated animals, slow firing neurons fired at a 55% and 46% higher rate during θ rhythm and LIA,

respectively, compared to controls. There was no significant difference between the mean firing rates of the PBS treated animals and the Aβ 40-1 treated animals (Figure 6, Table 2) Accumulative data is depicted in fig 6B.

3.6 Hippocampal theta rhythm is abnormal in the Aβ 1–40 treated rat

Power Spectrum analysis from the EEG recordings in the hippocampus of the three experimental groups showed that theta rhythm amplitude at peak frequency was altered in the Aβ 1–40 treated group. Theta rhythm amplitude was reduced 49% (54592 mV^2/Hz and 48989 mV^2/Hz in controls to 26514 mV^2/Hz in Aβ 1–40 treated animals, $p = 0.001$; Figure 6C–D) compared to controls. No significant difference in power amplitude was found between PBS and Aβ 40-1 controls.

3.7 Aβ 1–40 reduced the proportion of theta-correlated slow firing neurons

Examples of θ-correlated slow firing neurons from PBS, Aβ 40-1 and 1–40 are depicted in figure 7A, B and C, respectively. The percentage of θ-correlated slow firing neurons was significantly reduced by Aβ 1–40 septal injections. In the PBS and Aβ 40-1 treated groups, the percentage of recorded θ-correlated slow firing neurons was 35.6% (21/59) and 33.7% (16/49), respectively. In the Aβ 1–40 treated group, the percentage of recorded θ-correlated slow firing neurons was 04.0% (2/51). In comparison to controls, there was a significant reduction in the number of recorded θ-correlated slow firing neurons recorded in the Aβ 1–40 treated group (p =1 0.001)(Figure 7D). For all three experimental groups, no statistical differences were found in the fast firing group.

4. Discussion

The septo-hippocampal system is heavily affected in AD (Colom, 2006). Although Aβ is implicated in AD neurodegenerative processes, little is known about how it affects the function of specific septo-hippocampal networks. Furthermore, there are no studies correlating septo-hippocampal anatomical and functional alterations in AD or animal models of AD.

While Aβ has been extensively used *in vitro* as a neurotoxin (Colom et al., 1998, Butterfield, 2002, Chen, 2005, Jarvis et al., 2007, Liao et al., 2007), comparative few *in vivo* studies have been performed (Giovanelli *et al.*, 1995; Gonzalo-Ruiz *et al*., 2003; Gonzalo-Ruiz *et al*., 2006; Gonzales *et al*., 2007). Aβ has been applied *in vivo* using: (a) intraventricular injections and (b) local injections into defined brain structures. While the first approach has been used to study general effects (Nakamura *et al.*, 2001), the second has primarily been used to determine Aβ effects on specific neuronal populations (Giovanelli *et al.*, 1995; Gonzalo-Ruiz *et al*., 2003; Gonzalo-Ruiz *et al*., 2006; Gonzales *et al.*, 2007). Since the primary goal of this study was to investigate Aβ affects on a specific region of the basal forebrain, local injections of Aβ were utilized.

Our data demonstrates that local injections of Aβ into the medial septum damage both cholinergic and glutamatergic septal neuronal populations while sparing GABAergic neuronal populations. The use of an antibody against the structural protein NeuN confirms that the decrease in cholinergic and glutamatergic markers is due to a reduction in the population of septal neurons and not transitory injuries. Thus, our animal model mimics the pathology observed in humans with AD. While the vulnerability of cholinergic neurons to AD and Aβ has been extensively documented (Davies, 1976), the vulnerability of glutamatergic systems has only recently begun to be investigated (Francis *et al.*, 1999). Our data show that septal glutamatergic neurons are affected by Aβ. Our data also show that septal glutamatergic terminals (VGLUT2) and glutamatergic terminals with an extraseptal origin (VGLUT1) are affected by Aβ. Thus, the septal glutamatergic system and the circuits its neurons integrate are

highly vulnerable to Aβ. This Aβ-induced glutamatergic damage in addition to the Aβ induced cholinergic lesion may account for the septo-hippocampal physiological alterations observed in our analysis of Aβ actions.

Aβ altered septal networks and produced a change in hippocampal theta rhythm. Recordings of hippocampal theta rhythm in Aβ 1–40 treated rats displayed a significantly lower power/amplitude (49% reduction) when compared to recordings from rats injected with PBS and Aβ 40-1. The decrease in hippocampal theta amplitude suggests that the septal networks necessary for theta rhythm production and maintenance are altered by Aβ 1–40 injections in the medial-septum of rats. This reduction in the theta rhythm amplitude may be a consequence of the reduction in the number of theta-correlated slow firing septal neurons in the septo-hippocampal networks.

The occurrence of hippocampal theta rhythm is dependent upon the proportion of septal neurons involved in the rhythmic process. Furthermore, the frequency of the theta field activity is determined by the frequency of the rhythmical “theta” bursts in septal neurons (Bland and Colom, 1993; Vinogradova, 1995). Septal lesions abolish the hippocampal theta rhythm in rodents, providing further evidence of the importance of the septum in theta generation (Andersen *et al.*, 1979; Rawlins *et al.*, 1979; Winson, 1978). Thus, a reduction of septal cholinergic (57%) and glutamatergic (53%) neuronal populations plus a reduction of glutamatergic terminals (VGLUT1: 21%, VGLUT2: 40%) is sufficient to significantly alter the amplitude of hippocampal theta rhythm as well as the hippocampal functions that require neuronal synchronization at theta frequencies.

One possible reason for this alteration is that Aβ septal injections are acting at the hippocampal level through a reduction of acetylcholine release (Abe *et al.*, 1994). The diminished amount of acetylcholine may not be sufficient to appropriately synchronize hippocampal networks. Reduced septal glutamatergic influences most likely add to this effect. Theta frequency and amplitude are affected by lateral septum modulation of NMDA receptors (Puma *et al.*, 1996; Puma and Bizot, 1999, Bland *et al.*, 2007). Furthermore, the injection of NMDA receptor antagonists into the MS-DB significantly decreases hippocampal theta rhythm amplitude (Leung and Shen, 2004). Puma’s and Leung’s results in conjunction with our findings suggest that septal glutamatergic synapses play an important role in hippocampal theta rhythm generation. Deficit in glutamatergic synaptic transmission and synchronous network activity have been found in hippocampal slices from transgenic mice over expressing the human form of the amyloid precursor protein (APP) harboring the Swedish mutation (Brown *et al.*, 2005), suggesting that Aβ increases may lead to dysfunctional glutamatergic systems. In the medial septum bath application of Aβ (1–40 and 25–35) also depressed glutamatergic synaptic transmission (Santos-Torres *et al.*, 2007).

In contrast to the amplitude/power changes observed, the theta frequency was unchanged in recordings from Aβ-treated rats compared to control rats. This finding suggests that the surviving neurons and circuits are adequate to maintain oscillatory activities at theta frequencies and that basic generator mechanisms continue operating at the same pace in Aβ-treated rats. The exact mechanism underlying theta oscillations is still under debate (Colom, 2006). In Aβ treated animals, oscillations at theta frequencies may be produced by (a) surviving neurons of Aβ-altered septal circuits, (b) unaffected extra-septal networks or (c) both (Bland and Colom, 1993; Colom, 2006). Our data suggest that Aβ-induced reductions in theta power may be produced by the reduction in rhythmically firing septal neurons. Bassant’s group (Simon *et al.*, 2006) did not find septal cholinergic neurons correlated to the hippocampal theta rhythm in anesthetized and non-anesthetized *in vivo* preparations. Their work suggests that most rhythmical septal neurons are GABAergic or glutamatergic. Reduction of septal cholinergic and glutamatergic inputs onto GABAergic septal neurons may reduce the

population of rhythmically bursting GABAergic neurons. Although unaffected in numbers, the population of septal GABAergic neurons may be dysfunctional in Aβ-treated animals. Juxtacellular or intracellular recordings with identification of neuronal phenotypes are needed to clarify this issue.

At the unitary level slow firing neurons from Aβ-treated animals significantly increased their firing rates. This finding suggests that: (a) surviving slow firing neurons must increase their activity to support a reduced amplitude theta or (b) increased firing patterns are a direct result of Aβ-induced toxicity. Discerning between these two possibilities exceeds the scope of this study and will be the aim of future investigations in our laboratory. Slow firing septal cholinergic neurons have typically been considered important for theta generation (Yoder and Pang, 2005; Colom, 2006). This study shows that altered hippocampal theta is associated with altered slow firing patterns in septal neurons. Slow firing septal neurons, most likely cholinergic and glutamatergic (Sotty *et al.*, 2003; Manseau *et al.*, 2005), may provide a background of excitation for theta rhythm generation. This activity may be increased in the Aβ-injured brain to compensate for the septal neuronal loss. Thus, our data further supports the notion that slow firing septal neurons play a role in hippocampal theta rhythm generation.

Preliminary experiments not reported in this study using anti-VGLUT1 and anti-VGLUT2 antibodies in colchicine-treated rats revealed that VGLUT2 neurons constitute a larger neuronal population in the medial septum when compared to VGLUT1 neurons. Thus, numerous VGLUT2 terminals in the medial septum may originate from intraseptal VGLUT2 neurons, while VGLUT1 terminals might represent extraseptal VGLUT1 projections. These results suggest that reductions in VGLUT2 puncta may correspond to reductions in septal glutamate-immunoreactive neurons but reductions in VGLUT1 puncta represent lesions of septal terminals that originate in extraseptal glutamatergic populations. Thus, Aβ may injure both local circuits and circuits with extraseptal components.

Excitotoxic mechanisms have been implicated in cell death in AD (Gray and Patel, 1995). This is further supported by the neuroprotective effect of the NMDA antagonist memantine (Hynd *et al.*, 2004) in AD patients. The finding that glutamatergic septal neurons are susceptible to Aβ may indicate that Aβ affects the septum through excitotoxic mechanisms. The presence of functional NMDA receptors in septal neurons (Kumamoto and Murata, 1995) suggests that the machinery needed for excitotoxic processes is present in the septum. Some of the slow firing neurons recorded in this study were probably glutamatergic (Sotty *et al.*, 2003; Manseau *et al.*, 2005). Slow firing neurons showed increased firing rates following Aβ 1–40 treatment. Those alterations may be part of a process that leads to increases in glutamate release and excessive activation of NMDA receptors in Aβ-treated rats. This mechanism may lead to neurodegeneration and explain the reduction in slow firing neuronal numbers in our electrophysiological recordings as well as the reduced number of cholinergic and glutamatergic neurons in our anatomical experiments. Further studies are necessary to determine the mechanisms underlying Aβ-induced septal functional alterations and neuronal degeneration.

In conclusion, this study shows that cholinergic and glutamatergic septal neurons are vulnerable to Aβ and that glutamatergic circuits are injured in the presence of amyloid. This alteration in septal neuronal populations and circuitry results in abnormal hippocampal theta rhythms suggesting that these neurons and circuits are important in maintaining the amplitude of septo-hippocampal rhythmic activities at theta frequencies.

Acknowledgments

We thank Alicia Gonzalo-Ruiz for her valuable advice about Aβ preparation and administration. This study was supported by National Institutes of Health: Grants -1P20 MD0001091 and 5S06GM0688550-Dr. Luis V. Colom.

6. References

Abe E, Casamenti F, Giovannelli L, Scali C, Pepeu G. Administration of amyloid beta-peptides into the medial septum of rats decreases acetylcholine release from hippocampus in vivo. Brain Res 1994;636:162–164. [PubMed: 8156403]

Andersen P, Bland HB, Myhrer T, Schwartzkroin PA. Septo-hippocampal pathway necessary for dentate theta production. Brain Res 1979;165:13–22. [PubMed: 427577]

Bell KF, Ducatenzeiler A, Ribeiro-da-Silva A, Duff K, Bennett DA, Cuello AC. The amyloid pathology progresses in a neurotransmitter-specific manner. Neurobiol Aging 2006;27:1644–1657. [PubMed: 16271419]

Bland BH, Colom LV. Extrinsic and intrinsic properties underlying oscillation and synchrony in limbic cortex. Prog Neurobiol 1993;41:157–208. [PubMed: 8332751]

Bland BH, Oddie SD. Theta band oscillation and synchrony in the hippocampal formation and associated structures: the case for its role in sensorimotor integration. Behav Brain Res 2001;127:119–136. [PubMed: 11718888]

Bland BH, Oddie SD, Colom LV. Mechanisms of neural synchrony in the septohippocampal pathways underlying hippocampal theta generation. J Neurosci 1999;19:3223–3237. [PubMed: 10191335]

Bland BH, Declerck S, Jackson J, Glasgow S, Oddie S. Septohippocampal properties of N-methyl-D-asparate-induced theta-band oscillation and synchrony. Synapse 2007;61:185–197. [PubMed: 17173326]

Brazhnik ES, Fox SE. Intracellular recordings from medial septal neurons during hippocampal theta rhythm. Exp Brain Res 1997;114:442–453. [PubMed: 9187280]

Brazhnik ES, Fox SE. Action potentials and relations to the theta rhythm of medial septal neurons in vivo. Exp Brain Res 1999;127:244–258. [PubMed: 10452212]

Brown DR, Kozlowski H. Biological inorganic and bioinorganic chemistry of neurodegeneration based on prion and Alzheimer diseases. Dalton Trans 2004:1907–1917. [PubMed: 15252577]

Butterfield DA. Amyloid beta-peptide (1–42)-induced oxidative stress and neurotoxicity: implications for neurodegeneration in Alzheimer's disease brain. A review. Free Radic Res 2002;36:1307–1313. [PubMed: 12607822]

Caplan JB, Madsen JR, Schulze-Bonhage A, Aschenbrenner-Scheibe R, Newman EL, Kahana MJ. Human θ Oscillations Related to Sensorimotor Integration and Spatial Learning. J Neuroscience 2003;23:4726–4736.

Chen C. beta-Amyloid increases dendritic Ca2+ influx by inhibiting the A-type K+ current in hippocampal CA1 pyramidal neurons. Biochem Biophys Res Commun 2005;338:1913–1919. [PubMed: 16289381]

Colom LV. Septal networks: relevance to theta rhythm, epilepsy and Alzheimer's disease. J Neurochem 2006;96:609–623. [PubMed: 16405497]

Colom LV, Bland BH. Medial septal cell interactions in relation to hippocampal field activity and the effects of atropine. Hippocampus 1991;1:15–30. [PubMed: 1669341]

Colom LV, Castaneda MT, Reyna T, Hernandez S, Garrido-Sanabria E. Characterization of medial septal glutamatergic neurons and their projection to the hippocampus. Synapse 2005;58:151–164. [PubMed: 16108008]

Colom LV, Diaz ME, Beers DR, Neely A, Xie WJ, Appel SH. Role of potassium channels in amyloid-induced cell death. J Neurochem 1998;70:1925–1934. [PubMed: 9572276]

Colom LV, Garcia-Hernandez A, Castaneda MT, Perez-Cordova MG, Garrido-Sanabria ER. Septo-hippocampal networks in chronically epileptic rats: potential antiepileptic effects of theta rhythm generation. J Neurophysiol 2006;95:3645–3653. [PubMed: 16554504]

Davies P, Maloney AJ. Selective loss of central cholinergic neurons in Alzheimer's disease. Lancet 1976;2:1403. [PubMed: 63862]

Ekstrom AD, Caplan JB, HoE, Shattuck K, Fried I, Kahana MJ. Human Hippocampal Theta Activity During Virtual Navigation. Hippocampus 2005;15:881–889. [PubMed: 16114040]

Francis PT, Palmer AM, Snape M, Wilcock GK. The cholinergic hypothesis of Alzheimer's disease: a review of progress. J Neurol Neurosurg Psychiatry 1999;66:137–147. [PubMed: 10071091]

Garrido-Sanabria ER, Perez MG, Banuelos C, Reyna T, Hernandez S, Castaneda MT, Colom LV. Electrophysiological and morphological heterogeneity of slow firing neurons in medial septal/diagonal band complex as revealed by cluster analysis. Neuroscience 2007;146:931–945. [PubMed: 17412516]

Giovannelli L, Casamenti F, Scali C, Bartolini L, Pepeu G. Differential effects of amyloid peptides beta-(1–40) and beta-(25–35) injections into the rat nucleus basalis. Neuroscience 1995;66:781–792. [PubMed: 7651609]

Gonzalez I, Arevalo-Serrano J, Sanz-Anquela JM, Gonzalo-Ruiz A. Effects of beta-amyloid protein on M1 and M2 subtypes of muscarinic acetylcholine receptors in the medial septum-diagonal band complex of the rat: relationship with cholinergic, GABAergic, and calcium-binding protein perikarya. Acta Neuropathol 2007;113:637–651. [PubMed: 17294199]

Gonzalo-Ruiz A, Gonzalez I, Sanz-Anquela JM. Effects of beta-amyloid protein on serotoninergic, noradrenergic, and cholinergic markers in neurons of the pontomesencephalic tegmentum in the rat. J Chem Neuroanat 2003;26:153–169. [PubMed: 14615025]

Gonzalo-Ruiz A, Perez JL, Sanz JM, Geula C, Arevalo J. Effects of lipids and aging on the neurotoxicity and neuronal loss caused by intracerebral injections of the amyloid-beta peptide in the rat. Exp Neurol 2006;197:41–55. [PubMed: 16045911]

Gray CW, Patel AJ. Neurodegeneration mediated by glutamate and beta-amyloid peptide: a comparison and possible interaction. Brain Res 1995;691:169–179. [PubMed: 8590049]

Hajszan T, Alreja M, Leranth C. Intrinsic vesicular glutamate transporter 2-immunoreactive input to septohippocampal parvalbumin-containing neurons: novel glutamatergic local circuit cells. Hippocampus 2004;14:499–509. [PubMed: 15224985]

Hardy J, Selkoe DJ. The amyloid hypothesis of Alzheimer's disease: progress and problems on the road to therapeutics. Science 2002;297:353–356. [PubMed: 12130773]

Harkany T, De Jong GI, Soos K, Penke B, Luiten PG, Gulya K. Beta-amyloid (1–42) affects cholinergic but not parvalbumin-containing neurons in the septal complex of the rat. Brain Res 1995;698:270–274. [PubMed: 8581496]

Henderson Z, Morris NP, Grimwood P, Fiddler G, Yang HW, Appenteng K. Morphology of local axon collaterals of electrophysiologically characterised neurons in the rat medial septal/diagonal band complex. J Comp Neurol 2001;430:410–432. [PubMed: 11169477]

Huerta PT, Lisman JE. Heightened synaptic plasticity of hippocampal CA1 neurons during a cholinergically induced rhythmic state. Nature 1993;364:723–725. [PubMed: 8355787]

Hynd MR, Scott HL, Dodd PR. Glutamate-mediated excitotoxicity and neurodegeneration in Alzheimer's disease. Neurochem Int 2004;45:583–595. [PubMed: 15234100]

Jarvis K, Assis-Nascimento P, Mudd LM, Montague JR. Beta-amyloid toxicity and reversal in embryonic rat septal neurons. Neurosci Lett 2007;423:184–188. [PubMed: 17709203]

Jerusalinsky D, Kornisiuk E, Izquierdo I. Cholinergic neurotransmission and synaptic plasticity concerning memory processing. Neurochem Res 1997;22:507–515. [PubMed: 9130263]

Jones GA, Norris SK, Henderson Z. Conduction velocities and membrane properties of different classes of rat septohippocampal neurons recorded in vitro. J Physiol 1999;517(Pt 3):867–877. [PubMed: 10358125]

Kohler C, Chan-Palay V, Wu JY. Septal neurons containing glutamic acid decarboxylase immunoreactivity project to the hippocampal region in the rat brain. Anat Embryol (Berl) 1984;169:41–44. [PubMed: 6721220]

Kumamoto E, Murata Y. Excitatory amino acid-induced currents in rat septal cholinergic neurons in culture. Neuroscience 1995;69:477–493. [PubMed: 8552243]

Lee MG, Chrobak JJ, Sik A, Wiley RG, Buzsaki G. Hippocampal theta activity following selective lesion of the septal cholinergic system. Neuroscience 1994;62:1033–1047. [PubMed: 7845584]

Leung LS, Shen B. Glutamatergic synaptic transmission participates in generating the hippocampal EEG. Hippocampus 2004;14:510–525. [PubMed: 15224986]

Leung LW, Lopes da Silva FH, Wadman WJ. Spectral characteristics of the hippocampal EEG in the freely moving rat. Electroencephalogr Clin Neurophysiol 1982;54:203–219. [PubMed: 6179745]

Liao MQ, Tzeng YJ, Chang LY, Huang HB, Lin TH, Chyan CL, Chen YC. The correlation between neurotoxicity, aggregative ability and secondary structure studied by sequence truncated Abeta peptides. FEBS Lett 2007;581:1161–1165. [PubMed: 17328898]

Lynch G, Rose G, Gall C. Anatomical and functional aspects of the septo- hippocampal projections. Ciba Found Symp 1977:5–24. [PubMed: 83225]

Manseau F, Danik M, Williams S. A functional glutamatergic neurone network in the medial septum and diagonal band area. J Physiol 2005;566:865–884. [PubMed: 15919710]

McGee AW, Bredt DS. Assembly and plasticity of the glutamatergic postsynaptic specialization. Curr Opin Neurobiol 2003;13:111–118. [PubMed: 12593989]

Morales FR, Roig JA, Monti JM, Macadar O, Budelli R. Septal unit activity and hippocampal EEG during the sleep-wakefulness cycle of the rat. Physiol Behav 1971;6:563–567. [PubMed: 4337729]

Nakamura S, Murayama N, Noshita T, Annoura H, Ohno T. Progressive brain dysfunction following intracerebroventricular infusion of beta(1–42)-amyloid peptide. Brain Res 2001;912:128–136. [PubMed: 11532428]

O'Keefe J. Hippocampus, theta, and spatial memory. Curr Opin Neurobiol 1993;3:917–924. [PubMed: 8124075]

Pearson RC, Sofroniew MV, Cuello AC, Powell TP, Eckenstein F, Esiri MM, Wilcock GK. Persistence of cholinergic neurons in the basal nucleus in a brain with senile dementia of the Alzheimer's type demonstrated by immunohistochemical staining for choline acetyltransferase. Brain Res 1983;289:375–379. [PubMed: 6362777]

Puma C, Bizot JC. Hippocampal theta rhythm in anesthetized rats: role of AMPA glutamate receptors. Neuroreport 1999;10:2297–2300. [PubMed: 10439452]

Puma C, Monmaur V, Sharif A, Monmaur P. Intraseptal infusion of selective and competitive glutamate receptor agonist NMDA and antagonist D-2-amino-5-phosphonopentanoic acid spectral implications for the physostigmine-induced hippocampal theta rhythm in urethane-anesthetized rats. Exp Brain Res 1996;109:384–392. [PubMed: 8817268]

Rawlins JN, Feldon J, Gray JA. Septo-hippocampal connections and the hippocampal theta rhythm. Exp Brain Res 1979;37:49–63. [PubMed: 385334]

Santos-Torres J, Fuente A, Criado JM, Riolobos AS, Heredia M, Yajeya J. Glutamatergic synaptic depression by synthetic amyloid beta-peptide in the medial septum. J Neurosci Res 2007;85:634–648. [PubMed: 17171714]

Scali C, Prosperi C, Giovannelli L, Bianchi L, Pepeu G, Casamenti F. Beta(1–40) amyloid peptide injection into the nucleus basalis of rats induces microglia reaction and enhances cortical gamma-aminobutyric acid release in vivo. Brain Res 1999;831:319–321. [PubMed: 10412015]

Schliebs R. Basal forebrain cholinergic dysfunction in Alzheimer's disease--interrelationship with beta-amyloid, inflammation and neurotrophin signaling. Neurochem Res 2005;30:895–908. [PubMed: 16187224]

Selkoe DJ. Toward a comprehensive theory for Alzheimer's disease. Hypothesis: Alzheimer's disease is caused by the cerebral accumulation and cytotoxicity of amyloid beta-protein. Ann N Y Acad Sci 2000;924:17–25. [PubMed: 11193794]

Simon AP, Poindessous-Jazat F, Dutar P, Epelbaum J, Bassant MH. Firing properties of anatomically identified neurons in the medial septum of anesthetized and unanesthetized restrained rats. J Neurosci 2006;26:9038–9046. [PubMed: 16943562]

Sotty F, Danik M, Manseau F, Laplante F, Quirion R, Williams S. Distinct electrophysiological properties of glutamatergic, cholinergic and GABAergic rat septohippocampal neurons: novel implications for hippocampal rhythmicity. J Physiol 2003;551:927–943. [PubMed: 12865506]

Vinogradova OS. Expression, control, and probable functional significance of the neuronal theta-rhythm. Prog Neurobiol 1995;45:523–583. [PubMed: 7624485]

Whitehouse PJ, Price DL, Struble RG, Clark AW, Coyle JT, Delon MR. Alzheimer's disease and senile dementia: loss of neurons in the basal forebrain. Science 1982;215:1237–1239. [PubMed: 7058341]

Winson J. Loss of hippocampal theta rhythm results in spatial memory deficit in the rat. Science 1978;201:160–163. [PubMed: 663646]

Yoder RM, Pang KC. Involvement of GABAergic and cholinergic medial septal neurons in hippocampal theta rhythm. Hippocampus 2005;15:381–392. [PubMed: 15630696]

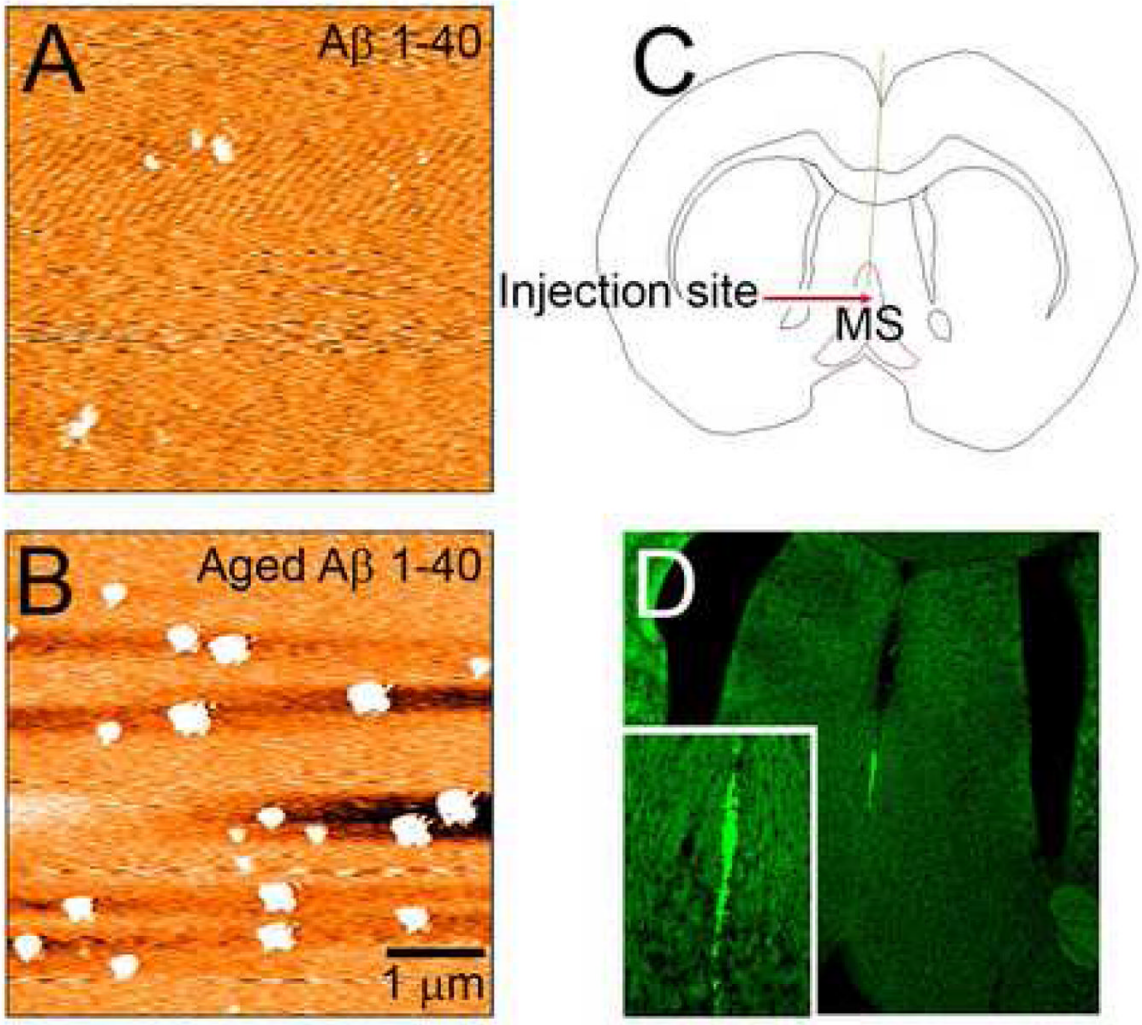

Figure 1.

A–B. Atomic force microscope (AFM) measurements showed minimum oligomerization in non-aged Aβ samples (A) and the presence of abundant oligomers in aged samples of Aβ 1–40 (B). C. Diagram depicting medial septum injection site. D. Fluorescent image of Thioflavine S in medial septum verifying presence of Aβ 1–40. Insert shows a magnified image of the injection, illustrating that Aβ is isolated to the medial septum. Only injections with minimal diffusion to adjacent areas were used.

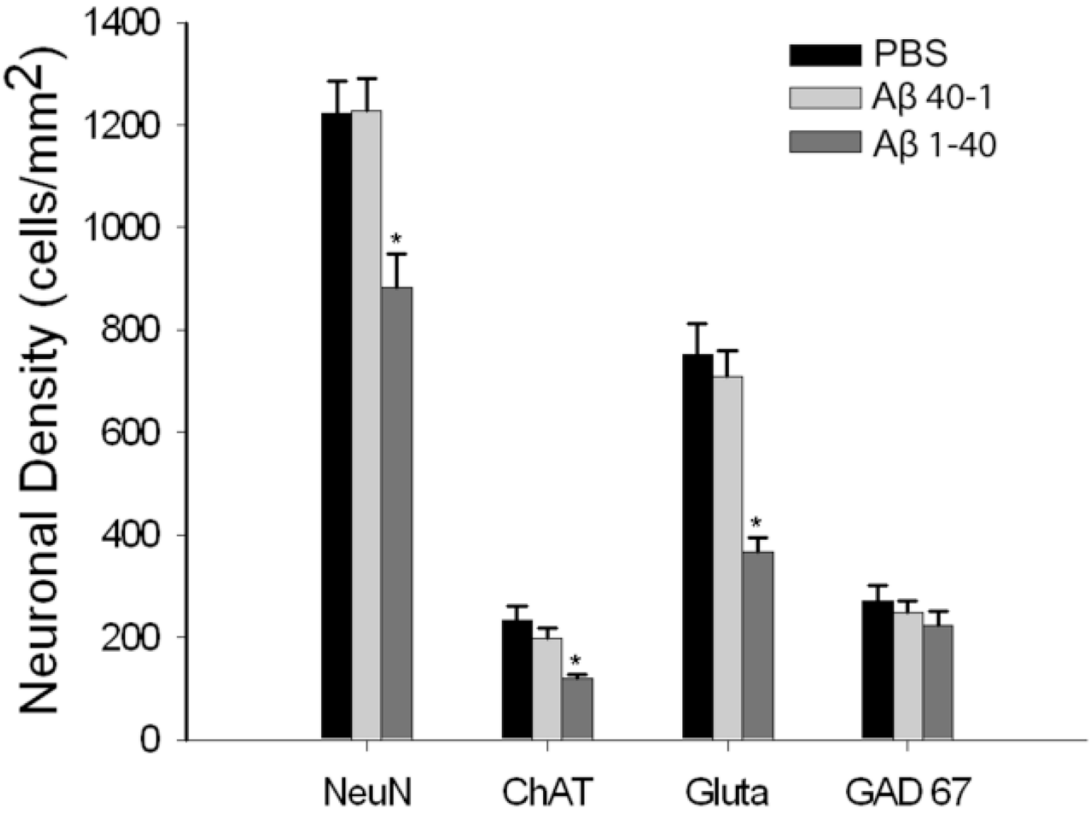

Figure 2.

Graph comparing the mean cell density of overall (NeuN), cholinergic (ChAT), glutamatergic (Gluta) and GABAergic (GABA) populations in the medial septum of PBS control rats, Aβ (40-1) control rats and Aβ 1–40 treated rats. Aβ 1–40 significantly reduced the overall number of medial septal neurons labeled by NeuN ($F_{[2,20]}$=4.69, p=0.02. While the numbers of both cholinergic ($F_{[2,32]}$ =11.2, p<0.01) and glutamatergic ($F_{[2,32]}$=2.32, p<0.01) neurons were significantly reduced GABAergic neurons were resistant to Aβ 1–40 (p>0.55). PBS or the reverse peptide did not produce significant alterations. *Statistically significant, *P*<0.05.

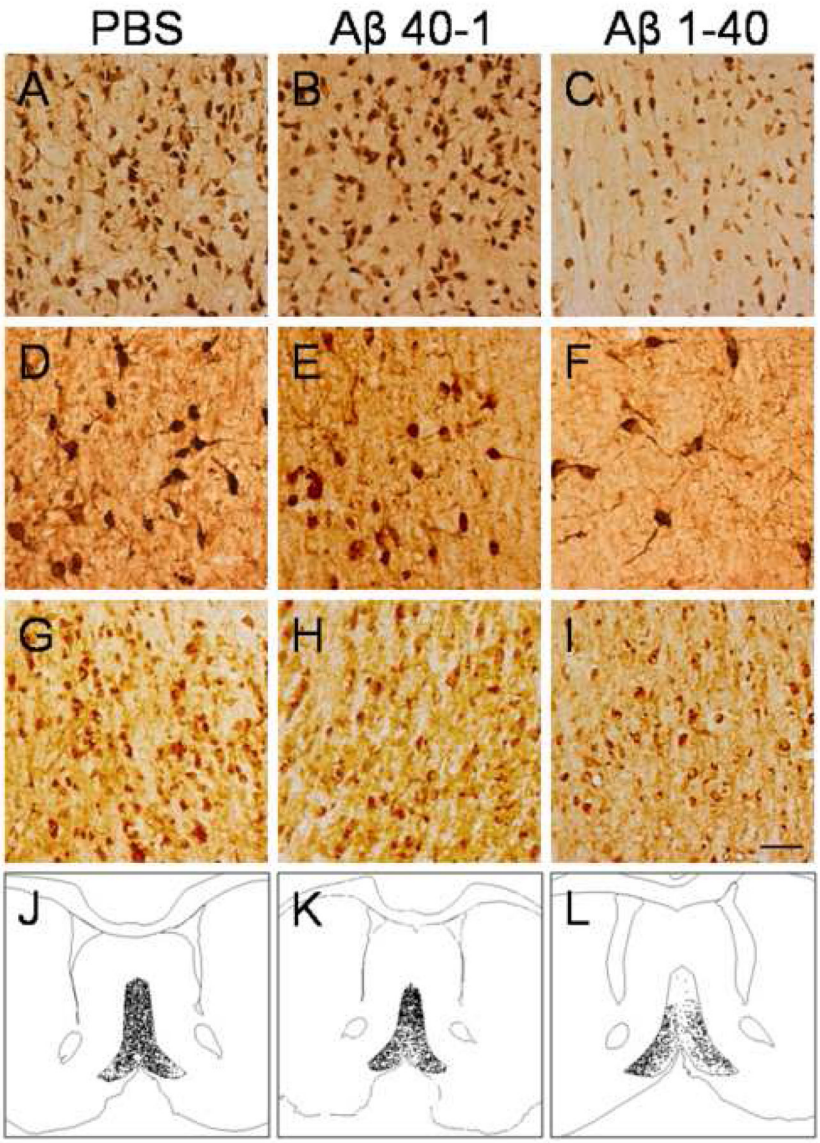

Figure 3.

Photomicrographs of NeuN (A–C), ChAT (D–F) and glutamate (G–I) immunoreactive neurons in the medial septum of PBS (A,D,G), Aβ 40-1 (B,E,H) and Aβ 1–40 (C,F,I) treated rats. Note the reduction in neuronal density in Aβ 1–40 treated tissue compared to control tissue. Panels J–L illustrate the reduction in glutamatergic cell density in PBS (J), Aβ 40-1 (K) and Aβ 1–40 (L) treated rats. Scale bar = 50 μm.

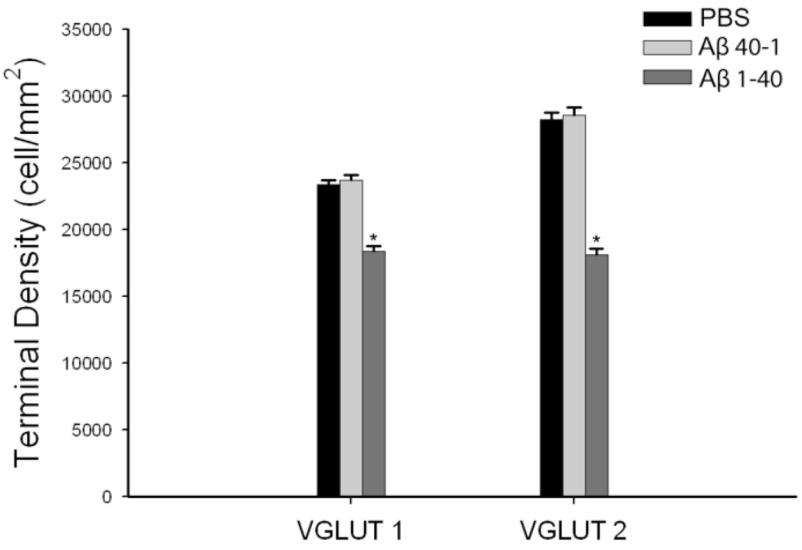

Figure 4.

Graph comparing the mean density of VGLUT1 and VGLUT2 puncta in the medial septum of PBS control rats (n=10), Aβ (40-1) control rats (n=6) and Aβ treated rats (n=10). In Aβ 40-1 treated tissue, terminal density in both VGLUT1 ($F_{[2,23]}$ =52.5, p<0.01) and VGLUT2 ($F_{[2,32]}$ =128.4, p<0.01) was significantly reduced. *Statistically significant, p<0.05.

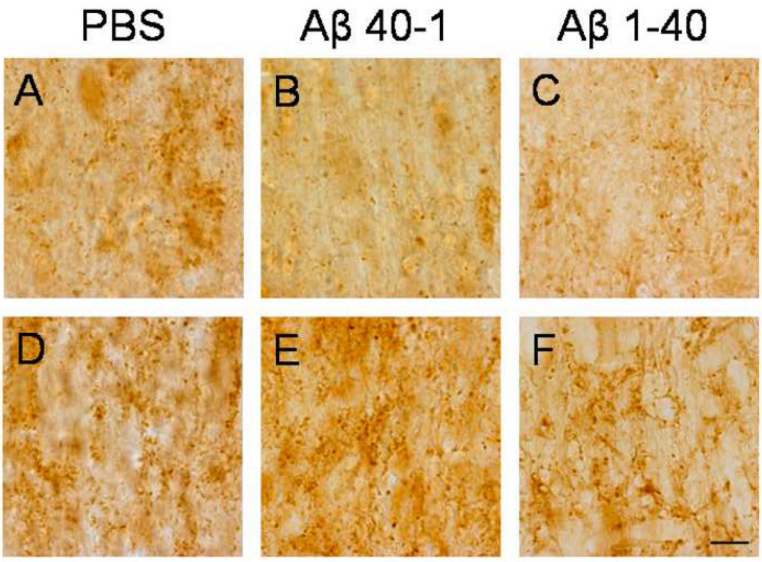

Figure 5.
Photomicrograph of VGLUT1 (A–C) and VGLUT2 (D–F) immunoreactive puncta in the medial septum of PBS (A, D), Aβ 40-1 (B, E) (n=6) and Aβ 1–40 (C, F) treated rats (n=10).

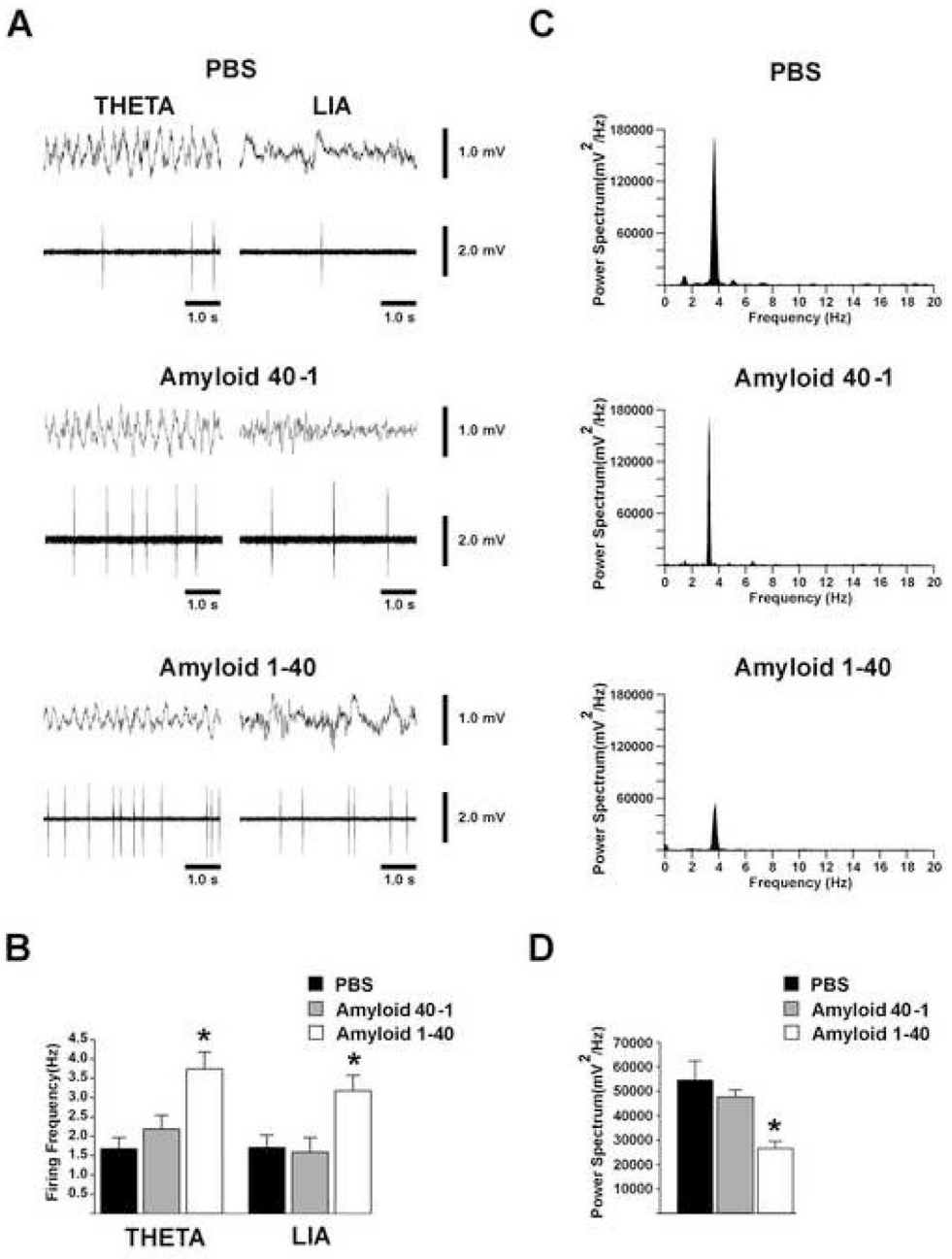

Figure 6.

A. Comparison of hippocampal field potentials (top trace) and firing patterns (bottom trace) of slow firing neurons (unit) from PBS, Aβ 40-1, and Aβ 1–40 treated animals. B. Bar graph depicting a significant increase in mean firing rates of slow firing neurons in Aβ 1–40 treated animals compared to controls. C. Graph of power spectrum of θ frequencies versus θ frequency of individual neurons illustrating that tail pinch induced robust field potential oscillations in controls but lowered the θ amplitude in Aβ 1–40 treated animals. D. Graph indicating power spectrum of recorded θ field potentials from Aβ 1–40 treated animals is significantly less than that of control. *Statistically significant, $p<0.05$.

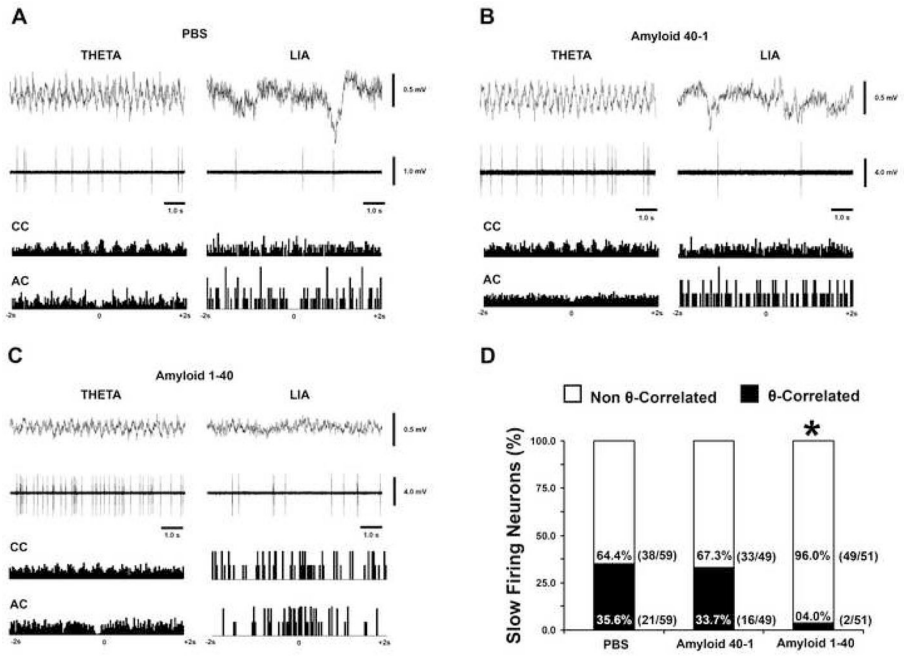

Figure 7.

A–C. Slow firing unit recordings (second trace) during θ and LIA episodes. Time histograms show neurons cross-correlated and auto-correlated with hippocampal field potentials during θ and LIA. D. Bar graph comparing non θ–correlated and θ–correlated slow firing neurons in Aβ 1–40, PBS and Aβ 40-1 treated groups. Slow firing neurons correlated with hippocampal θ rhythm decreased by 96.0% after septal injections of Aβ 1–40. In the PBS and Aβ 40-1 treated groups, recordings of slow firing neurons correlated to hippocampal θ rhythm were 35.6% and 33.7%, respectively. Compared to controls, there was a significant reduction in the number of slow firing neurons correlated to hippocampal theta rhythm in the Aβ 1–40 treated group. *Statistically significant, $p<0.05$.

Table 1

Mean cell densities of neuronal populations within the MS of PBS control rats, Aβ 40-1 control rats and Aβ 1–40 treated rats using ANOVA.

Phenotype	PBS (cell/mm^2)	Aβ 40-1 (cell/mm^2)	Aβ 1–40 (cell/mm^2)
NeuN*	(n = 5) 1261.8 ± 164.1	(n = 6) 1240.5 ± 137.7	(n = 12) 910.1 ± 48.5
ChAT*	(n = 11) 287.9 ± 47.7	(n = 6) 246.3 ± 24.1	(n = 18) 122.4 ± 9.2
GAD67	(n = 11) 273.5 ± 29.3	(n = 6) 248.5 ± 23.0	(n = 17) 232.2 ± 26.1
Gluta*	(n = 11) 770.3 ± 64.1	(n = 6) 710.2 ± 42.0	(n = 18) 362.7 ± 31.0

* Statistically significant, $p<0.05$.

Table 2

Mean firing rates of different neuronal firing patterns during Θ rhythm and LIA.

	PBS (n=69) (spikes/sec)	Aβ 40-1 (n=53) (spikes/sec)	Aβ 1–40 (n=61) (spikes/sec)
Slow firing			
Θ Correlated	k = 21	k = 16	k = 2
Firing rate at Θ*	2.90 ± 0.54	4.03 ± 0.64	5.00 ± 0.80
Firing rate at LIA*	2.57 ± 0.63	2.04 ± 0.42	1.00 ± 0.40
Non Θ Correlated	k = 38	k = 33	k = 49
Firing rate at Θ*	1.15 ± 0.32	1.58 ± 0.39	3.93 ± 0.46
Firing rate at LIA*	1.61 ± 0.42	1.41 ± 0.53	3.55 ± 0.42
Fast Firing			
Θ Correlated	k = 4	k = 1	k = 2
Firing rate at Θ	19.55 ± 3.31	21.20	19.00 ± 3.80
Firing rate at LIA	11.35 ± 2.00	4.80	15.80 ± 9.80
Non Θ Correlated	k = 6	k = 3	k = 8
Firing rate at Θ	19.66 ± 2.46	29.27 ± 7.62	19.11 ± 2.41
Firing rate at LIA	15.87 ± 3.85	20.73 ± 5.39	18.97 ± 5.36

*Statistically significant, $p<0.05$.